Radio diagnostics of electron shock acceleration in the corona at LOFAR frequencies

Nicolina Chrysaphi

CNES/LESIA – Observatoire de Paris, Meudon, France

Based on: Chrysaphi, N., Kontar, E. P., Holman, G. D., & Temmer, M. 2018, ApJ, 868, 79
Chrysaphi, N., Reid, H. A. S., & Kontar, E. P. 2020, ApJ, 893, 115

SolFER Spring 2021 Meeting
26 May 2021

nicolina.chrysaphi@obspm.fr

Type II Solar Radio Bursts

N. Chrysaphi (2021), PhD thesis, University of Glasgow

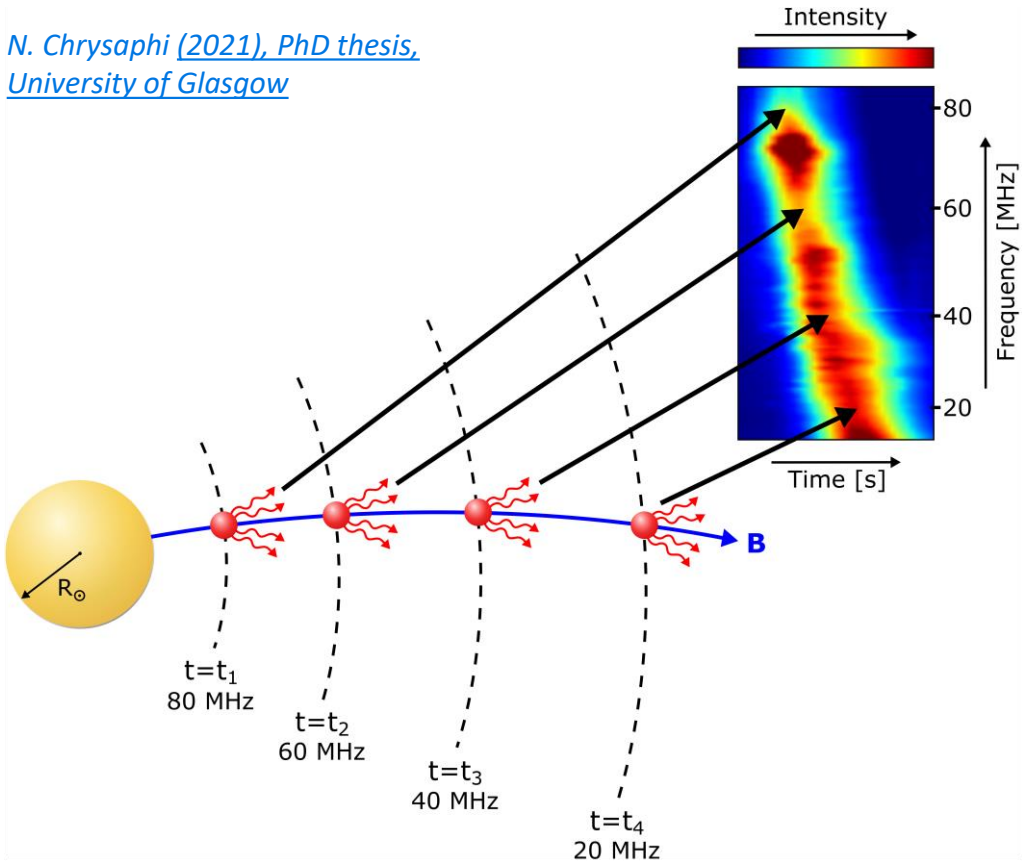

- **frequency relates to distance**

$\Longrightarrow f \propto \sqrt{n(r)}$, where f = frequency
n = plasma density
r = radial distance

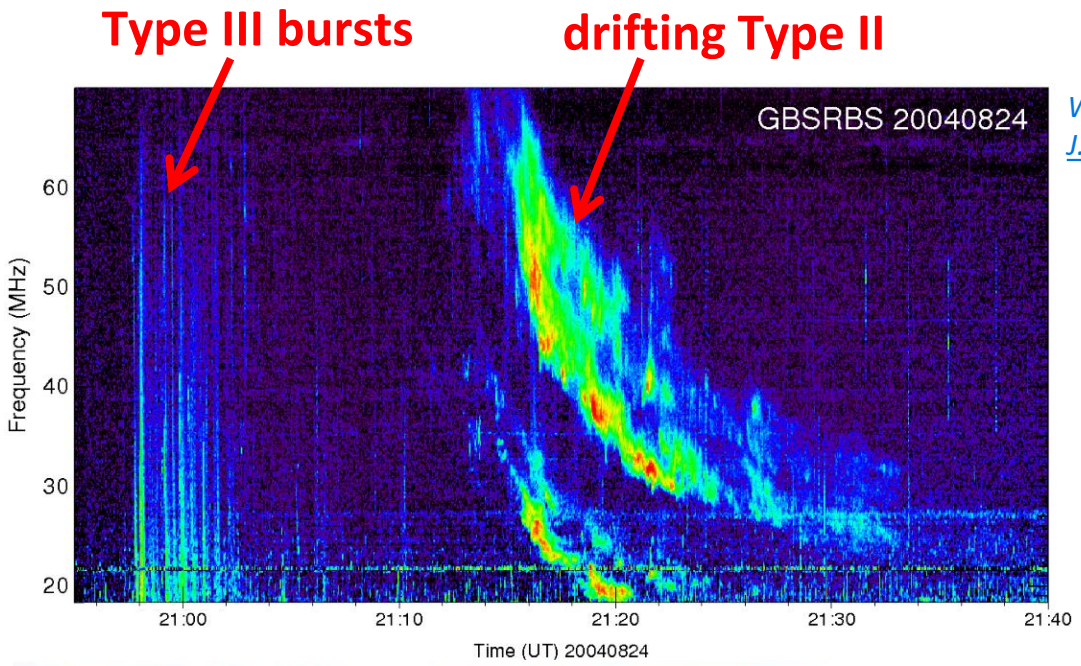

White 2007, Asian J. Phys., 16, 189

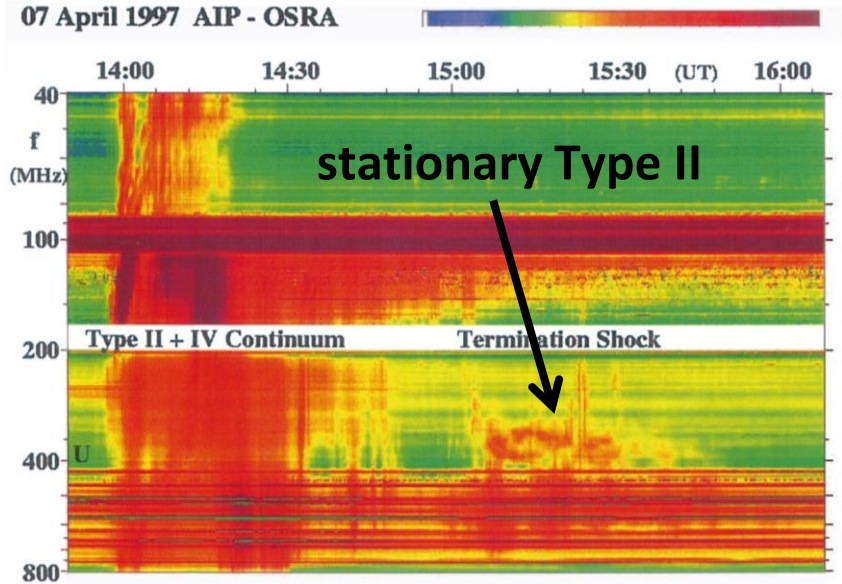

Aurass et al. 2002, A&A, 384, 273

Drifting Type II bursts:

- Excited by shock waves
  $\Longrightarrow$ linked to CMEs

Stationary Type II bursts:

- Associated to termination shocks in solar flares

nicolina.chrysaphi@obspm.fr

Transitioning Type II burst

Chrysaphi et al. 2020, ApJ, 893, 115

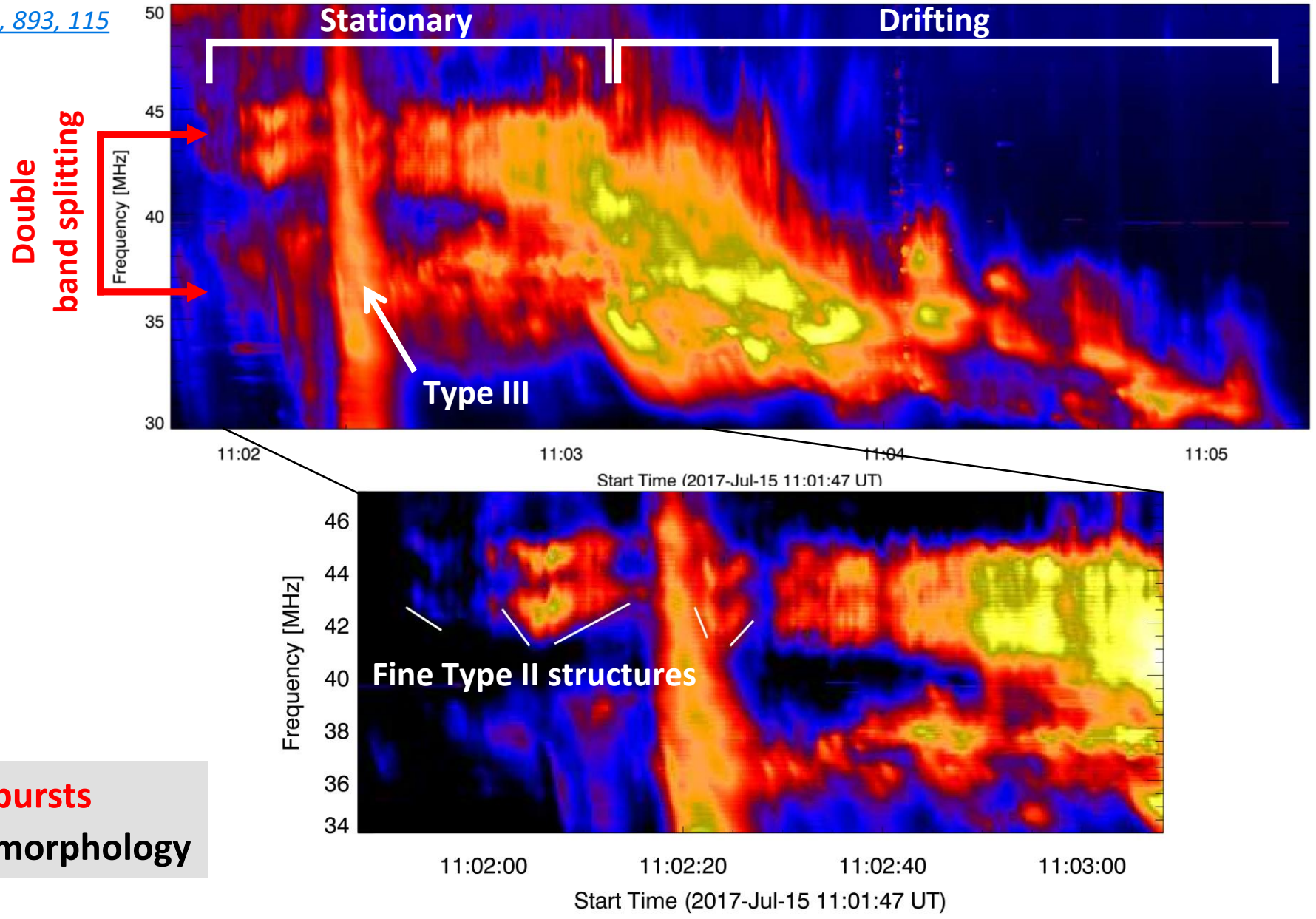

LOFAR Observations:

- Transition from stationary to drifting emissions
- Band-splitting
- Positive and negative frequency-drift fine structures

  ⟹ Duration: a few seconds

New sub-class of Type II bursts

Aim: Identify what causes this morphology

nicolina.chrysaphi@obspm.fr

Jet eruption and Streamer-puff CME

- 2 CME fronts, different behaviours, but both resulting from a bifurcated jet spire
- Type II emissions related to a streamer-puff CME
  ⟹ traces the streamer, inflates it, but leaves it intact

Chrysaphi et al. 2020, ApJ, 893, 115

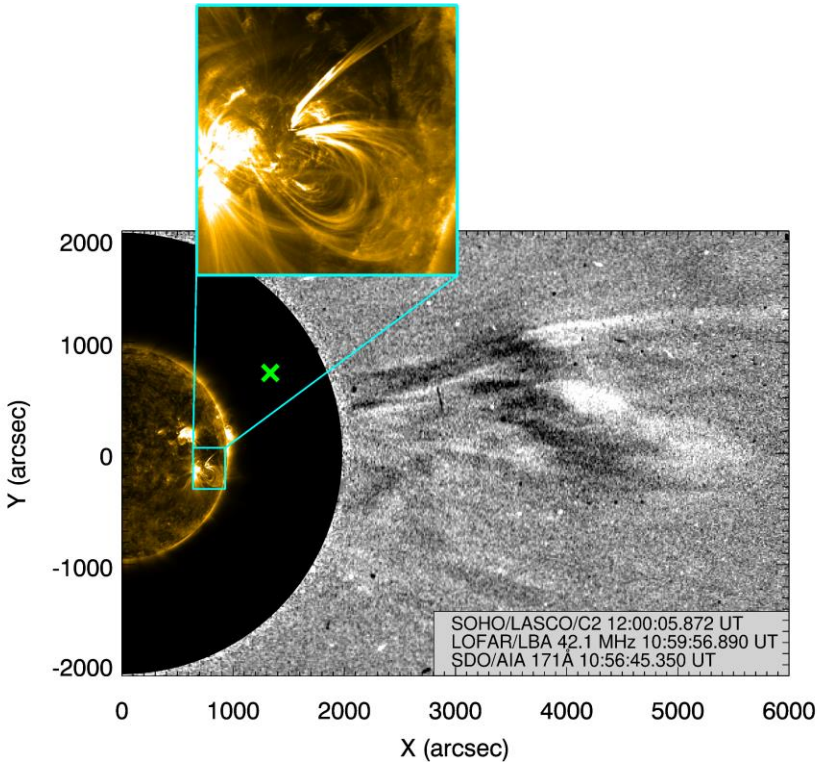

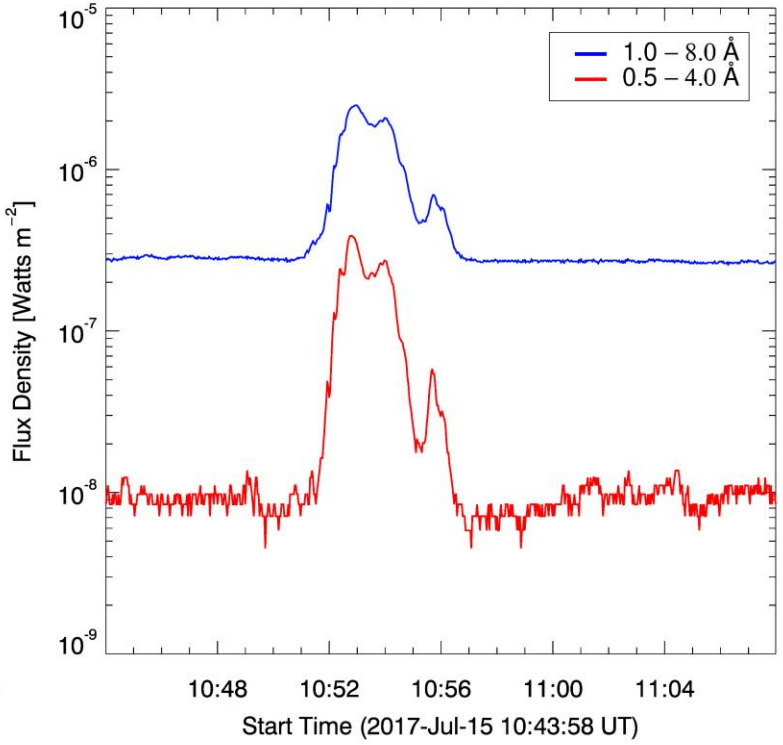

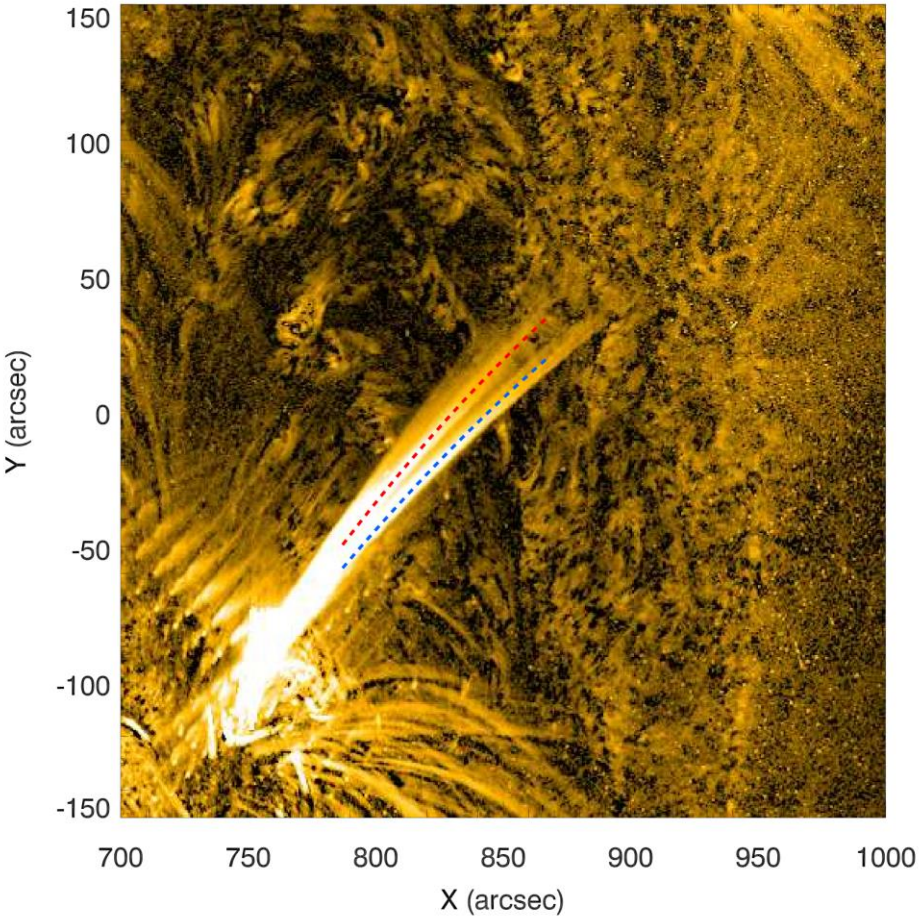

nicolina.chrysaphi@obspm.fr

LOFAR tied-array imaging

High resolution imaging spectroscopy:

- Temporal resolution ~ 0.01 s
- Spectral resolution ~ 12.2 kHz
- Spatial resolution ~ 10 arcmin at 30 MHz
- Sensitivity $\lesssim 0.03$ sfu per beam

Utilising LOFAR imaging:

- Examine the behaviour of the Type II sources before, during, and after the *transition time*

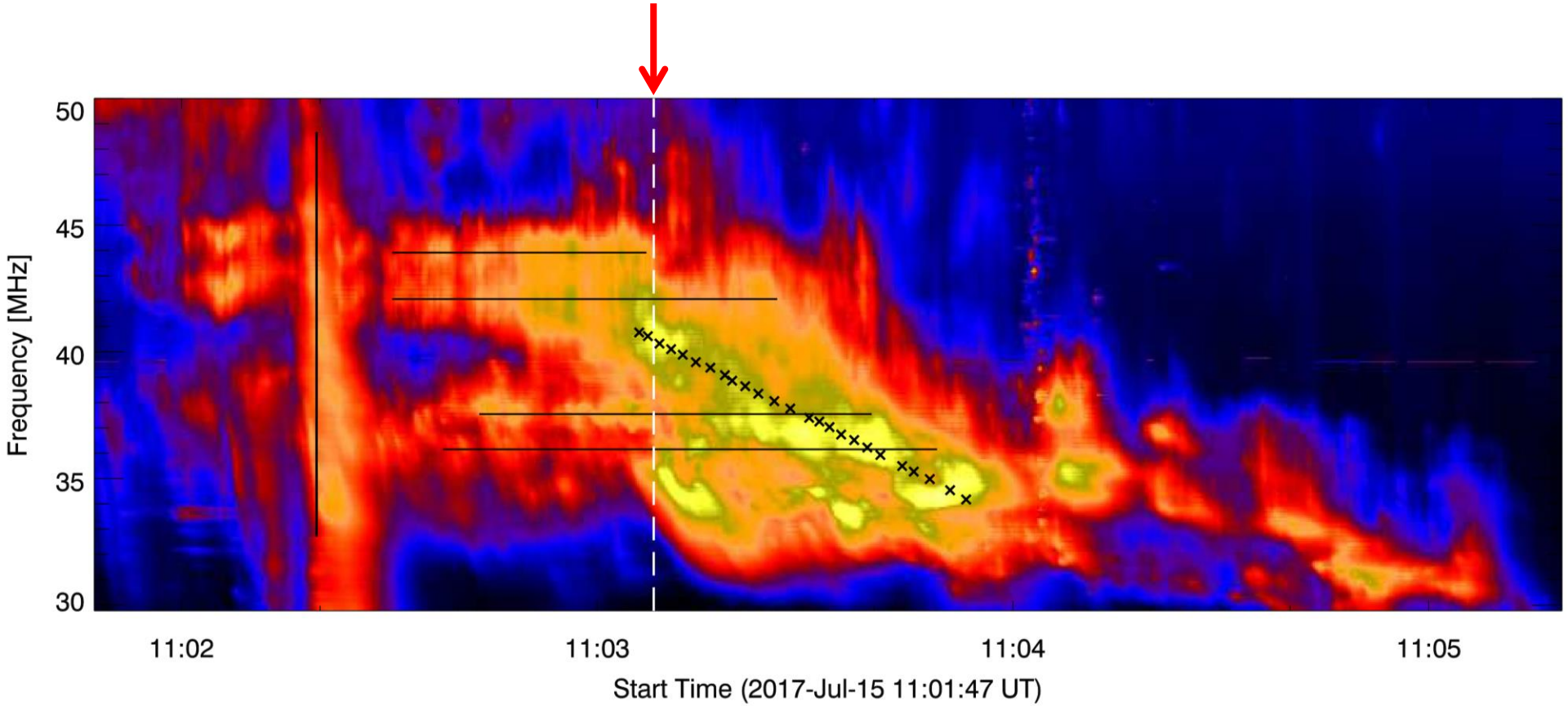

Chrysaphi et al. 2020, ApJ, 893, 115

nicolina.chrysaphi@obspm.fr

LOFAR imaging

Type II sources:

- "Jump" at transition time
- Stationary emissions move towards the solar centre (possibly due to projection effects)

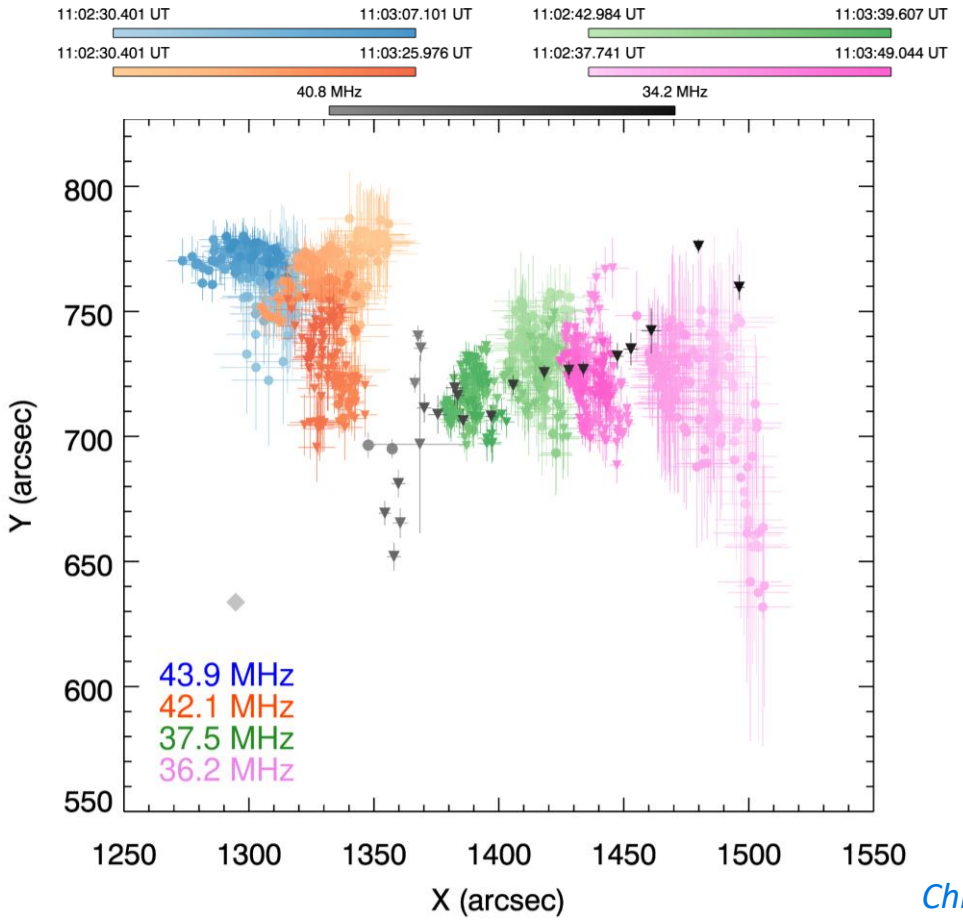

Type III sources:

- Unusual source pattern observed ⟹ abrupt changes in position
- Positional changes coincide with bandwidth of highest-frequency stationary Type II subbands (39 – 45 MHz)

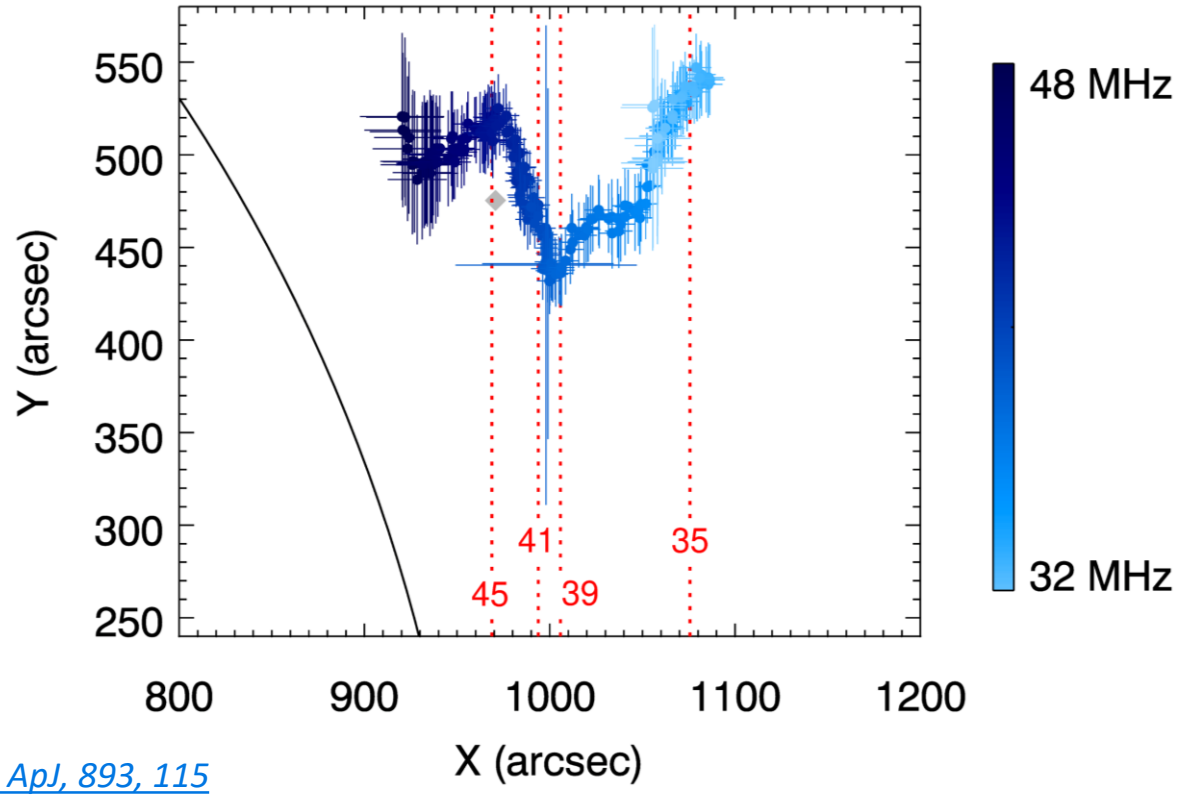

Chrysaphi et al. 2020, ApJ, 893, 115

nicolina.chrysaphi@obspm.fr

Proposed Generation Mechanism

- Jet eruption ⟹ streamer-puff CME ⟹ **transitioning Type II burst**
- Stationary Type II ⟹ streamer momentarily halts the shock front which acts as a standing shock
- Type II fine structures ⟹ CME-streamer interplay causing pulsations
- Type III ⟹ electron beam traces a magnetic field confining the locally-inflated streamer
- Drifting Type II ⟹ streamer succumbs to expansion, "jumps" to new location, but still compressed by shock

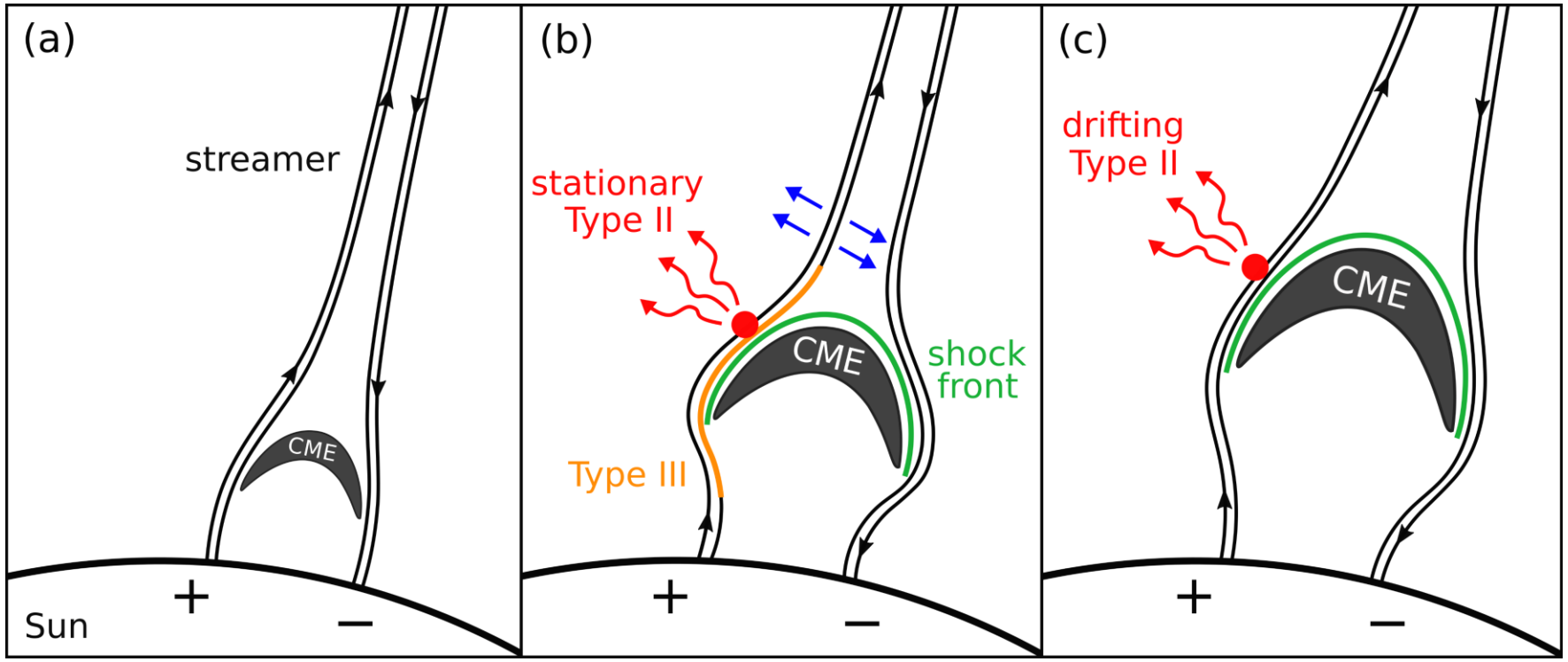

Chrysaphi et al. 2020, ApJ, 893, 115

nicolina.chrysaphi@obspm.fr

Simultaneous Type II subband imaging

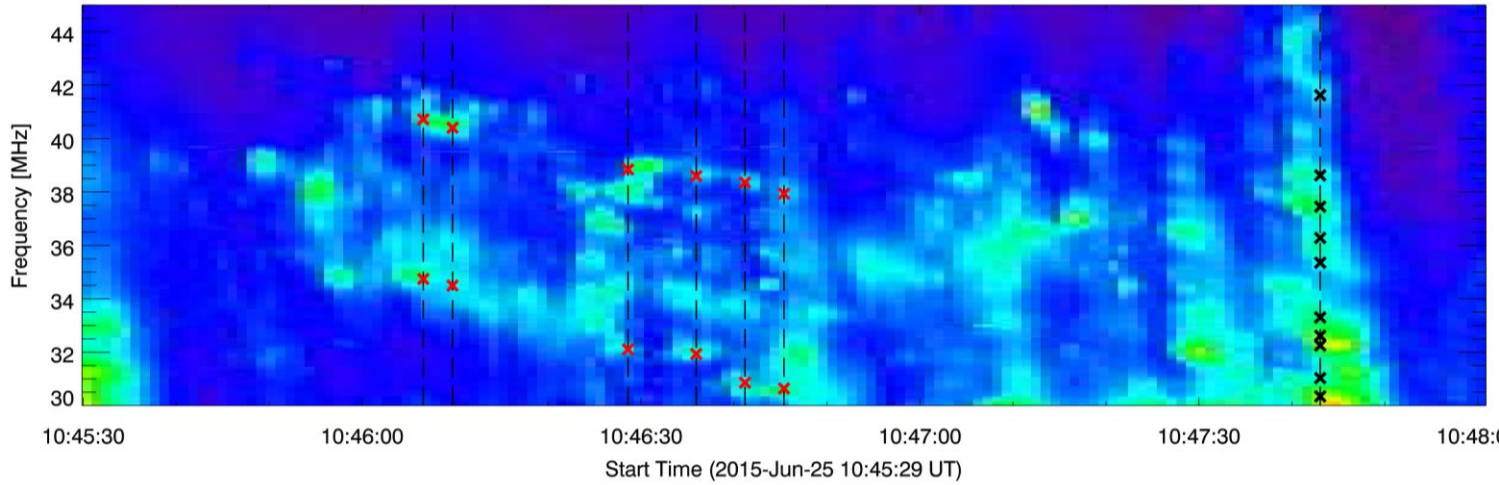

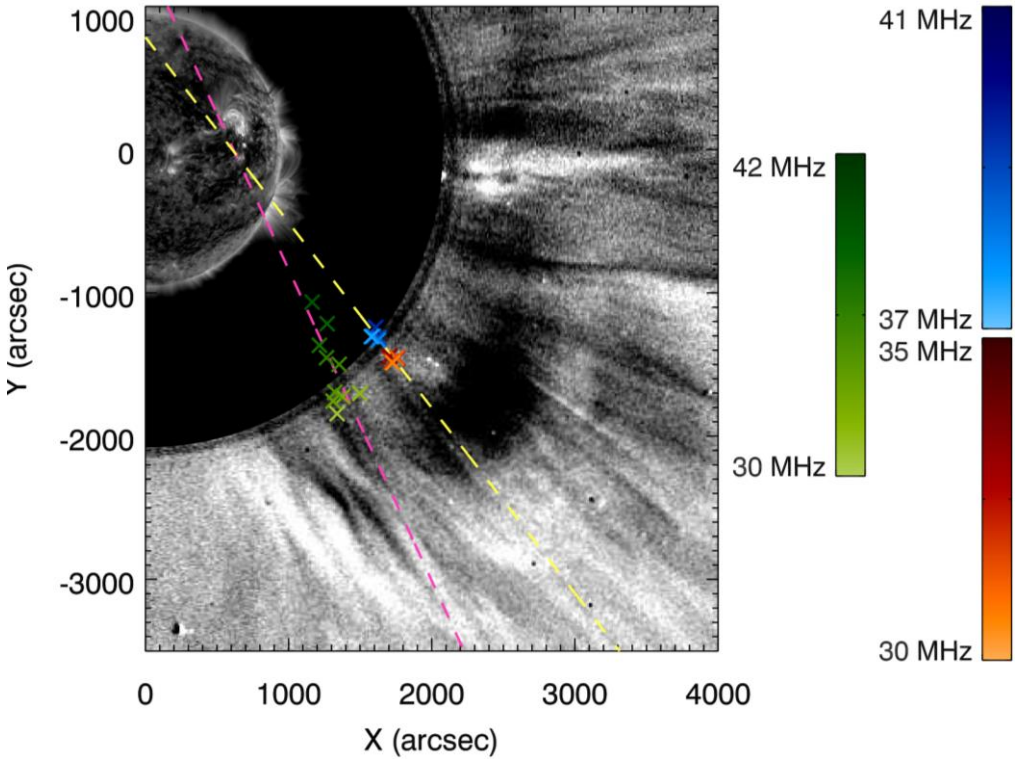

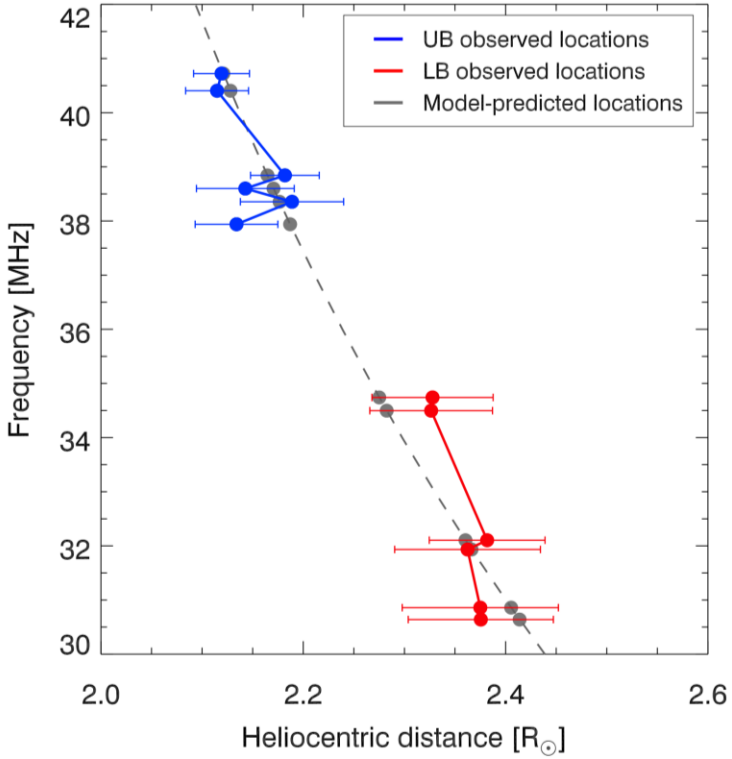

LOFAR Observations:

- Band-splitting
- First simultaneous imaging of both subbands
- Probe the emission locations of the subband sources

  ⟹ Debated for decades

- Observed average separation between the upper and lower subbands is $0.2 \pm 0.05\ \mathrm{R}_\odot$
- Observed locations best matched by the 4.5xNewkirk (1961) model

Chrysaphi et al. 2018, ApJ, 868, 79

nicolina.chrysaphi@obspm.fr

Radio-wave Scattering

- Density inhomogeneities in the corona affect the propagation of photons ⟹ scattering dominates

  (*Kontar et al. 2017, NatCo, 8, 1515; Kuznetsov et al. 2020, ApJ, 898, 94*)

- Lower frequencies scatter more:

$$\mu^2 \propto 1 - \frac{1}{f^2}$$ (where μ = refractive index)

Because of scattering:

- sources shift away from true position
- sources broaden

Message:

Radio observations do not reflect the true conditions at the emission excitation location

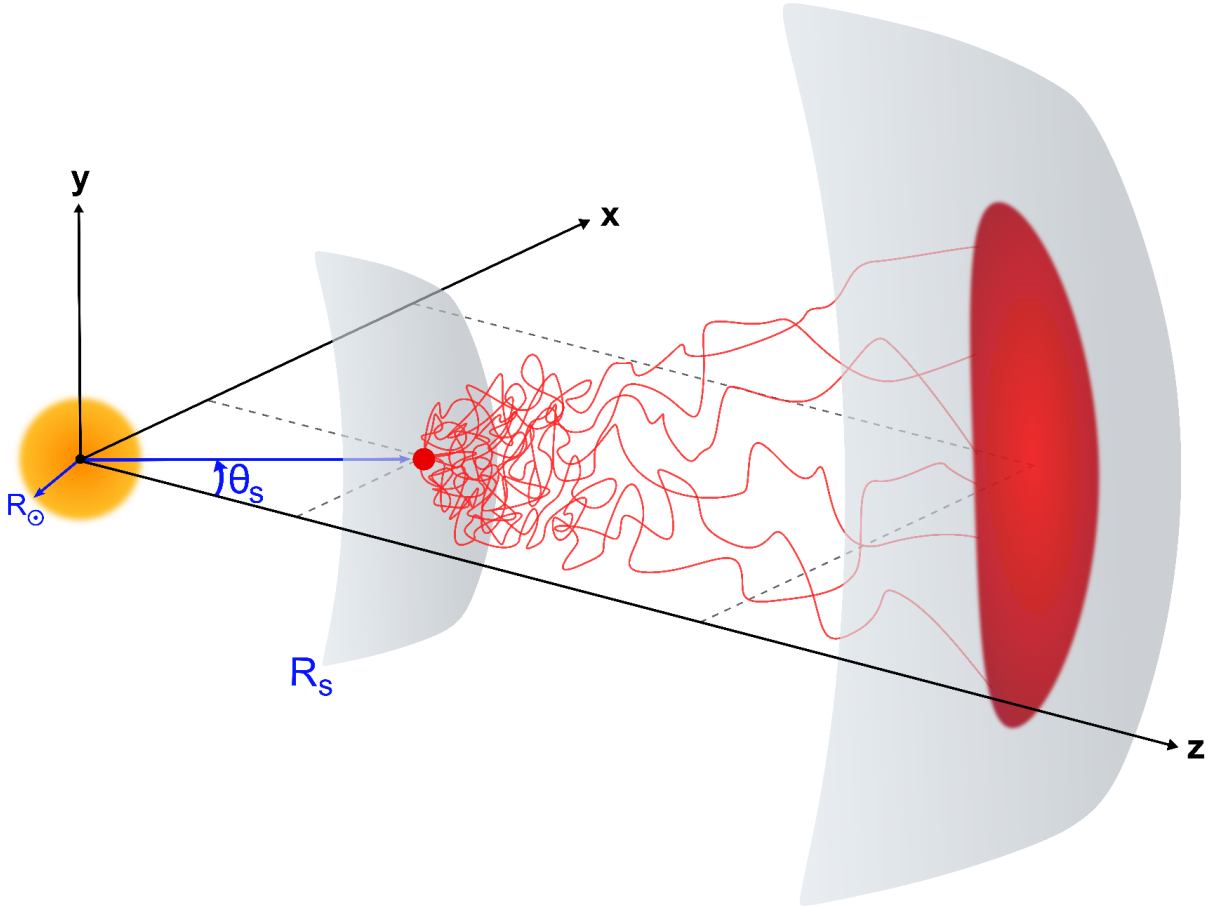

Kontar et al. 2019, ApJ, 884, 122

nicolina.chrysaphi@obspm.fr

Estimating the scattering-induced shift

- Derived an analytical expression for estimating the scattering-induced shift:

$$\tau(r) = \int_r^{1AU} \frac{d\langle \Delta\theta^2 \rangle}{dr} dr = \int_r^{1AU} \frac{\sqrt{\pi}}{2} \frac{f_{pe}^4(r)}{\left(f^2 - f_{pe}^2(r)\right)^2} \frac{\varepsilon^2}{h} dr$$

- A 40 MHz source shifts by 0.3 $R_\odot$ from true location, but a 32 MHz source shifts by 0.6 $R_\odot$

- A source at 32 MHz shifts by 0.3 $R_\odot$ away from a 40 MHz source

$\Longrightarrow$ Imaged separation of 0.2 ± 0.05 $R_\odot$ results from scattering of the radio waves

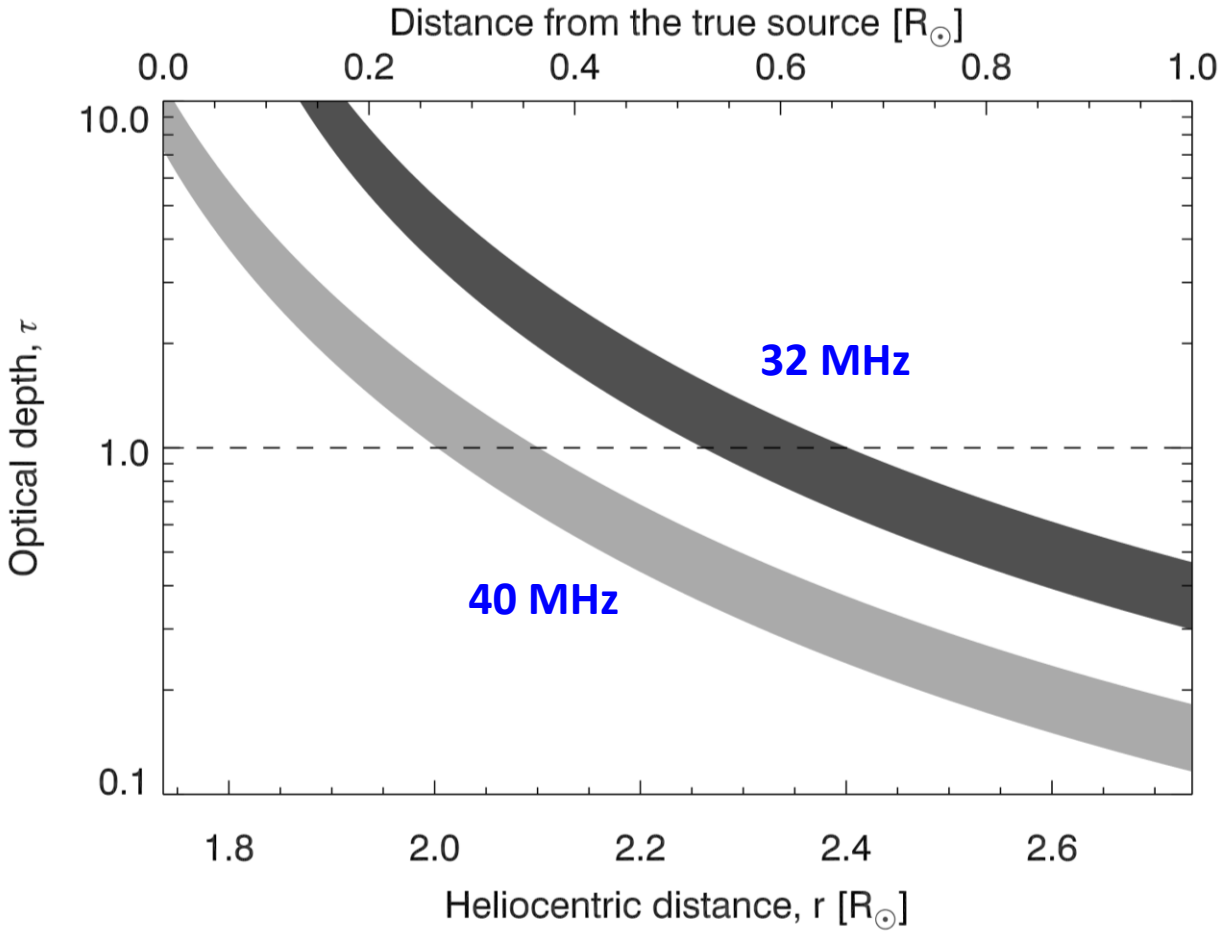

Chrysaphi et al. 2018, ApJ, 868, 79

nicolina.chrysaphi@obspm.fr

Results

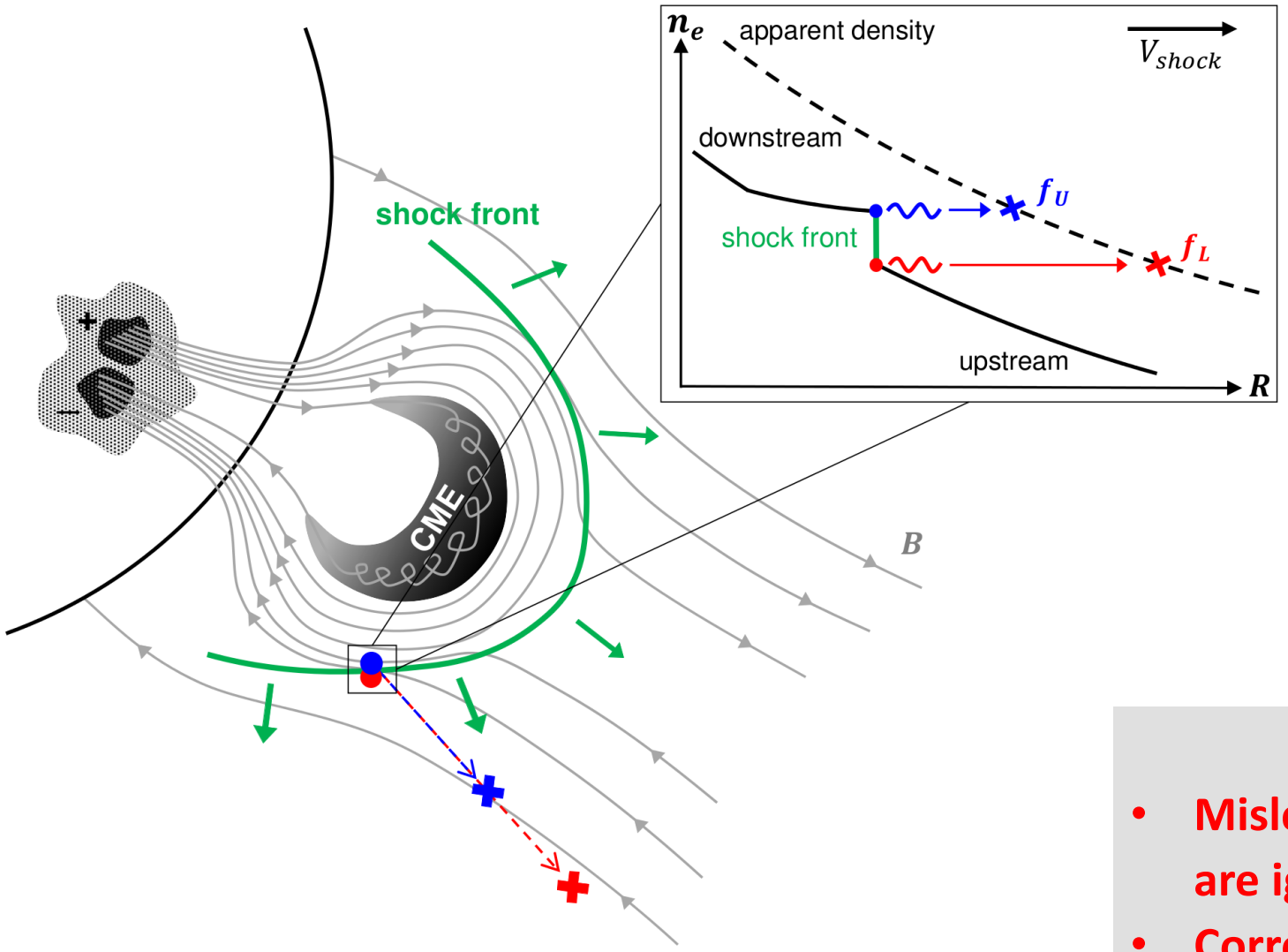

- Sources **appear separated due to scattering**, but intrinsic sources are **co-spatial**
- Shift correction **lowers the** apparent coronal **density by a factor of 4.3**

Main Conclusions:

- **Misleading interpretations if scattering effects are ignored**
- **Correction necessary for localising the origins of emissions sources**

Chrysaphi et al. 2018, ApJ, 868, 79

nicolina.chrysaphi@obspm.fr

Conclusions

Highlights:

- First observation of a transitioning Type II burst
- Related to a jet eruption and a streamer-puff CME
- Not attributed to a flare termination shock

- First simultaneous Type II subband imaging
- Consideration of scattering effects for split-band sources
- Different interpretation when scattering effects are considered: sources which are observed as separated could be **co-spatial**

Chrysaphi et al. 2018, ApJ, 868, 79; Chrysaphi et al. 2020, ApJ, 893, 115